

UC Irvine

UC Irvine Previously Published Works

Title

Integrated IVUS-OCT Catheter for in Vivo Intravascular Imaging

Permalink

<https://escholarship.org/uc/item/4439k6gg>

ISBN

978-1-4673-4561-3

Authors

Li, Xiang

Li, Jiawen

Jing, Joe

et al.

Publication Date

2012-10-01

DOI

10.1109/ultsym.2012.0391

Copyright Information

This work is made available under the terms of a Creative Commons Attribution License, available at <https://creativecommons.org/licenses/by/4.0/>

Peer reviewed

Integrated IVUS-OCT Catheter for *In Vivo* Intravascular Imaging

Xiang Li,¹ Jiawen Li,² Joe Jing,² Teng Ma,¹ Dilbahar Mohar,³ Aidan Raney,³ Sari Mahon,⁴ Matthew Brenner,⁴ Pranav Patel,³ K. Kirk Shung,¹ Zhongping Chen,^{2,5,6} and Qifa Zhou¹

¹ NIH Ultrasonic Transducer Resource Center and Department of Biomedical Engineering, University of Southern California, Los Angeles, CA 90089 USA

² Department of Biomedical Engineering, University of California, Irvine, Irvine, CA 92697 USA

³ Division of Cardiology, University of California, Irvine Medical Center, Orange, CA 92868 USA

⁴ Division of Pulmonary and Critical Care, University of California, Irvine Medical Center, Orange, CA 92868 USA

⁵ Edwards Lifesciences Center for Advanced Cardiovascular Technology, University of California, Irvine, Irvine, CA 92697 USA

⁶ Beckman Laser Institute, University of California, Irvine, Irvine, CA 92697 USA

Abstract - For the diagnosis of atherosclerosis, biomedical imaging techniques such as intravascular ultrasound (IVUS) and optical coherence tomography (OCT) have been developed. The combined use of IVUS and OCT is hypothesized to remarkably increase diagnostic accuracy. We report our progress on the probe design and imaging system for achieving a miniature catheter that is capable for *in vivo* animal study. The integrated IVUS-OCT catheter is featured by a sequential arrangement of an ultrasound transducer and an OCT probe. The capability of the integrated IVUS-OCT imaging catheter and system is demonstrated by *in vitro* and *in vivo* imaging experiments of rabbit abdominal aorta.

Keywords- IVUS; OCT; Intravascular

I. INTRODUCTION

Atherosclerosis is a complex syndrome characterized by plaque builds up on the inner lining of arteries, which is the leading cause of morbidity in developed countries. It has been proved that the vulnerable plaque which is composed of thin cap and lipid pool is life-threatening and responsible for the acute coronary syndromes (ACS).¹ Conventional method for diagnosing the vulnerability of plaque is the 20-40 MHz

intravascular ultrasound (IVUS) imaging, which is capable to visualize the structure of vessel wall with large penetration depth and moderate resolution. IVUS can resolve certain plaque and lipid pool; however, the image contrast and resolution might be insufficient to distinguish the complex constituents in vulnerable plaque.²⁻⁴ Optical Coherence Tomography (OCT) possesses superior resolution and is useful for detecting extremely thin plaque cap. However, the major limitation of OCT is the shallow penetration depth, which is around 1-2 mm.⁴⁻⁶ The complimentary properties suggest that an integrated imaging catheter and imaging system combining the two modalities would be more beneficial than either alone.

Previously, our group has developed different types of integrated intravascular imaging probes combining IVUS with OCT.⁷⁻¹⁰ In this paper, we report on a miniature integrated catheter and improvement of the whole system. The capability of our integrated IVUS-OCT catheter and imaging system is demonstrated by *in vitro* and *in vivo* imaging of rabbit abdominal aorta.

II. METHODS AND MATERIALS

A. Integrated IVUS-OCT Imaging system

The integrated IVUS-OCT imaging system is composed of four components: IVUS subsystem; OCT subsystem; motion control and coupling device; and data acquisition/processing unit. The frame rate of the imaging system is up to 20 frames per second with 500 A-lines per revolution and 8192 sampling points in each A-line. The system is capable for real time displaying and raw data saving. Pull-back speed is adjustable, 0.5-1 mm/s. In the OCT subsystem, the axial and lateral resolutions are optimized and measured to be 8 μm and 30 μm and the working distance is 3 mm. In the IVUS subsystem, the axial and lateral resolutions are measured to be 57 μm and 275 μm for using 40 MH transducers and working distance is over 7 mm. A photograph of the system is shown in Fig.1.

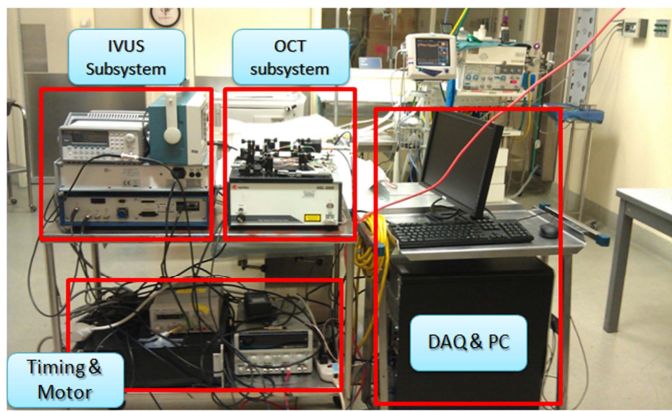


Fig.1 A photograph of the integrated IVUS-OCT system

In the IVUS subsystem, a Panametrics PR5900 pulser/receiver (Olympus NDT, Inc., Kennewick, WA) is used to excite the transducer and also receive the echo signals. Two μJ pulse energy is used to drive the transducer. 26 dB gain as well as 10-100 MHz band-pass filter is applied to the received RF signal.

In the swept-source OCT (SS-OCT) subsystem, light from a SS (center wavelength, 1310 nm; FWHM bandwidth, 100 nm; output power, 2.7 mW; scanning rate, 20 KHz; Santec Corp., Komaki, Aichi, Japan) is split by an 80/20 1 \times 2 coupler, with 80% of the power directed to the IVUS-OCT probe and the remaining 20% to the reference arm. Two circulators are used in both arms to redirect back-scattered and back-reflected

light to the two input ports of a 50/50 2 \times 2 coupler for balanced detection.

The light source generates 20 KHz trigger signals which drive a function generator (Agilent Technologies, Inc., Santa Clara, CA) serving as a frequency divider to provide up to 10 KHz triggers to synchronize the data acquisition board and the pulser/receiver. Both IVUS and OCT signals are digitized by a two-channel, 12 bit data acquisition board (Alazar Technologies Inc., Pointe-Claire, QC, Canada) working at a sampling rate of 200 MHz. The 200 MHz clock is provided by an external voltage controlled oscillator. The acquired IVUS and OCT signals are processed, saved and displayed by a custom built program in real time.

A custom built rotary joint device is used for motion control and signal coupling from the rotational part to the stationary part. The rotational motor (Animatics, Santa Clara, CA, USA) is mounted to a gear fixture with gear ratio of 2:1. A fiber optic rotary joint (Princeton, Inc., Pennington, New Jersey) and an electrical slip ring (Prosperous, Co., Hangzhou, China) are used for signal coupling. All these components are fixed to a translational stepper motor which functions for imaging pull-back.

B. Integrated IVUS-OCT catheter

The schematic of the distal end of the miniature IVUS-OCT catheter is shown in Fig.2, which features a sequential arrangement of the IVUS transducer and OCT probe. Within the OCT probe, a 0.35 mm-diameter gradient index (GRIN) lens (NSG America, Inc., Somerset, NJ) is used for light focusing, followed by a 0.3 mm-diameter micro-prism (Tower Optical Corp., Boynton Beach, FL) for reflecting the focused light beam into tissue. All the optical components are fixed in a polyimide tube with an outer diameter of 0.41 mm and wall thickness of 0.025 mm (Small Parts, Inc., Miramar, FL). The working distance of the OCT probe is about 3 mm. The ultrasonic transducer with an aperture size of 0.4 mm \times 0.4 mm is built using a PMN-PT single crystal (H.C. Materials, Bolingbrook, IL) which has superior piezoelectric properties

for building high sensitivity ultrasound transducers in a small size. The center frequency of the ultrasound transducer is 40 MHz with a fractional bandwidth of 52%. The two way insertion loss is measured to be 15 dB at the center frequency. The transducer is fixed in a thin-wall stainless tube (OD 0.64 mm, wall thickness 0.051 mm, Cadence, Inc., Staunton, VA) within which the OCT probe is also fixed. A window is made on the tube to let both the light beam and acoustic wave exit. Finally, the transducer wire and optical fiber are confined in a double wound flexible torque coil with an outer diameter of 0.65 mm. It is known beforehand that the transducer and prism are 2 mm apart, thus coregistered OCT and IVUS images can easily be matched from the 3D pull-back data sets by offsetting OCT and IVUS images at this distance. The catheter is more than 1.6 m long, with the maximum outer diameter of 0.65 mm, which can be fit in a 3.6 Fr catheter sheath for *in vivo* animal study.

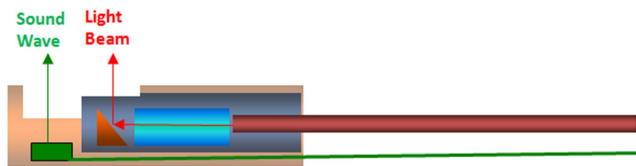


Fig.2 The schematic of the distal end of the miniature IVUS-OCT catheter

C. Imaging on rabbit model of atherosclerosis

To test the miniature catheter’s capability, we conducted *in vitro* and *in vivo* imaging on rabbit abdominal aorta. The atherosclerotic plaque model was built from New Zealand white rabbits. The rabbits were first undergone a balloon surgery, and then placed on a high-cholesterol diet for over 4 months. Segments of the rabbit abdominal aortas were harvested freshly for *in vitro* imaging. The imaged segments were pinpointed and fixed in formalin after imaging for Hematoxylin-Eosin (H&E) stained histology examination. In the *in vivo* experiment, a healthy rabbit was anesthetized and incubated during the surgical and imaging procedures. The rabbit was cut open chest, then the imaging catheter was inserted from thoracic aorta down to the abdominal aorta. Imaging pullback and saline flushing for blood clearance was

performed. The integrated IVUS-OCT catheter was spinning within a 3.6 Fr catheter sheath (Boston Scientific Corp., Natick, MA) to avoid contamination and causing trauma to the vessel wall.

III. RESULTS

A. In Vitro Experiment

In vitro IVUS and OCT images acquired from the integrated IVUS-OCT catheter on a segment of rabbit aorta is shown in Fig.3. The histology result [Fig.3 (c)] shows eccentric fibrous plaque on the left panel, while the intima on the right panel is not significantly thickened. The IVUS image [Fig.3 (b)] clearly distinguishes the thickened intima from the media layer on the left panel. The entire plaque is identified in the IVUS image. In the OCT image [Fig.3 (a)], the intima on the right panel appears thin and relatively moderate in brightness. On the left panel, OCT signal is strong at surface but diffused inside the plaque, which demonstrates a typical characteristic of fibrous plaque. Due to the superior resolution, the fibrous plaque in OCT image displays two layers. The bright boarder (yellow arrow) of the fibrous plaque in OCT image represents a fibrous plaque cap, which is also seen in histology [Fig.3 (c)] as a very thin but darker boarder (black arrow) on the surface of plaque. However, this feature is not detected in IVUS image due to the inferior resolution.

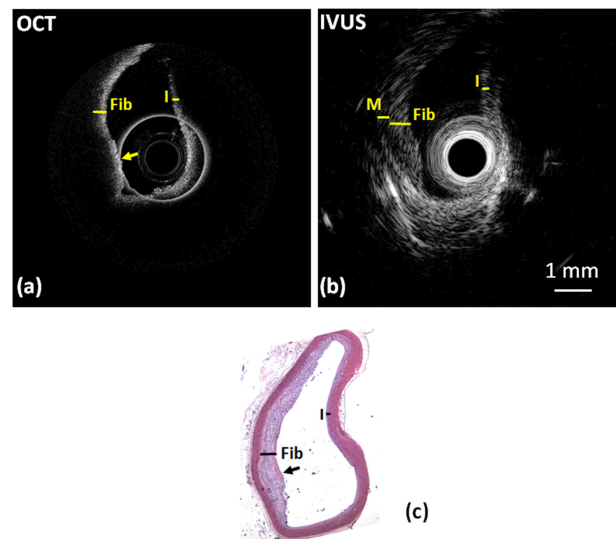


Fig.3 OCT (a), IVUS (b) and corresponding H&E histology (c) images of an atherosclerotic rabbit aorta with eccentric plaque. I, intima; M, media; Fib, fibrous plaque. The yellow and black arrows point to a plaque cap in OCT and histology images, respectively

B. In Vivo Experiment

In vivo imaging of normal rabbit abdominal aorta was performed using this miniature catheter and integrated system. Fig.4 (a) and (b) shows the OCT and IVUS images without flushing. Since blood is highly scattering for OCT but serves as natural transmission media for IVUS, no vessel structure can be seen in OCT image [Fig.4 (a)] but clearly visualized in IVUS image [Fig.4 (b)]. When applying flushing agent, a clear view was obtained for OCT as shown in Fig.4 (c). The fused image as shown in Fig.4 (e) shows that the OCT and IVUS images match well. We can see fine resolution of the aorta surface in the OCT image, and deep penetration depth into the aortic wall in the US image.

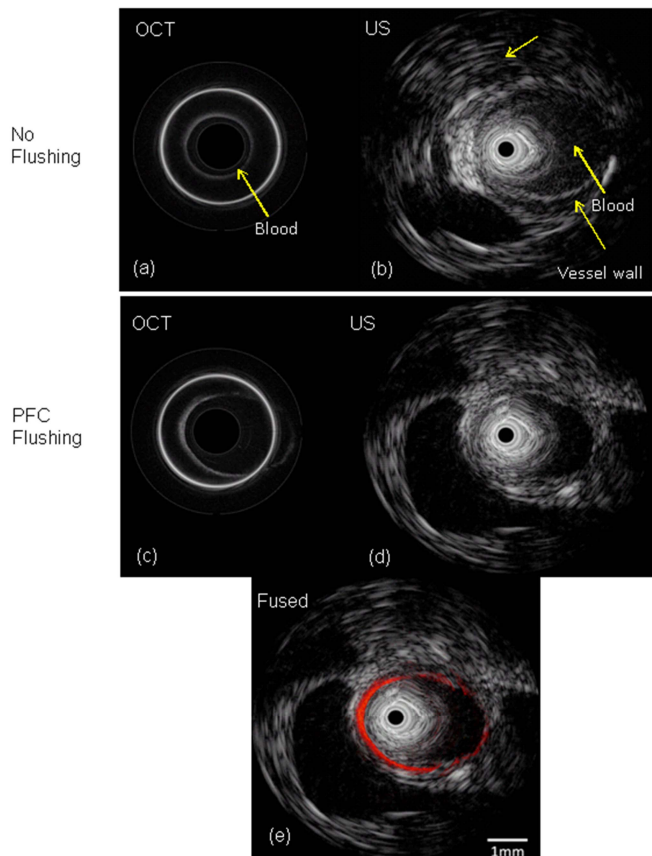


Fig.4 OCT (a) and ultrasound (b) images of rabbit abdominal aorta without flushing. OCT (c), ultrasound (d) and combined (e) OCT-US images with flushing

IV. CONCLUSION

We have successfully developed a miniature integrated IVUS-OCT catheter and imaging system which is suitable for intravascular imaging. *In vitro* and *in vivo* imaging of rabbit model demonstrates the feasibility of our catheter and system

for intravascular imaging. The results of these experiments hold promise for this integrated modality to be used in clinical study, providing high resolution and high penetration depth for better assessment of vulnerable plaque.

ACKNOWLEDGMENT

We would like to thank Ms. Tanya Burney, Mr. David Yoon and Mr. Earl Steward for their assistance during the surgical procedure. The project described was supported by NIH (UL1 RR031985, R01EB10090, R01EB-00293, R01HL105215, RR-01192, and P41-EB2182) and the U.S. Air Force Office of Scientific Research, Medical Free-Electron Laser Program FA9550-08-1-0384. Institutional support from the Beckman Laser Institute Endowment is also gratefully acknowledged.

REFERENCES

- [1] S. Rathore, M. Terashima, H. Matsuo, Y. Kinoshita, M. Kimura, E. Tsuchikane, K. Nasu, M. Ehara, Y. Asakura, O. Katoh, and T. Suzuki, "In-vivo detection of the frequency and distribution of thin-cap fibroatheroma and ruptured plaques in patients with coronary artery disease: an optical coherence tomographic study," *Coron Artery Dis.* **22**(1), 64-72 (2011).
- [2] G. Pasterkamp, E. Falk, H. Woutman, and C. Borst, "Techniques characterizing the coronary atherosclerotic plaque: Influence on clinical decision making," *J. Am. Coll. Cardiol.* **36**, 13-21 (2000).
- [3] F. S. Foster, C. J. Pavlin, K. A. Harasiewicz, D. A. Christopher, and D. H. Turnbull, "Advances in ultrasound biomicroscopy," *Ultrasound Med. Biol.* **26**(1), 1-27 (2000).
- [4] T. Sawada, J. Shite, H. M. Garcia-Garcia, T. Shinke, S. Watanabe, H. Otake, D. Matsumoto, Y. Tanino, D. Ogasawara, H. Kawamori, H. Kato, N. Miyoshi, M. Yokoyama, P. W. Serruys, and K. Hirata, "Feasibility of combined use of intravascular ultrasound radiofrequency data analysis and optical coherence tomography for detecting thin-cap fibroatheroma," *Eur. Heart J.* **29**, 1136-1146 (2008).
- [5] R. Puri, M. I. Worthley, and S. J. Nicholls, "Intravascular imaging of vulnerable coronary plaque: current and future concepts," *Nat. Rev. Cardiol.* **8**(3), 131-139 (2011).
- [6] P. Patwari, N. J. Weissman, S. A. Boppart, C. Jesser, D. Stamper, J. G. Fujimoto, and M. E. Brezinski, "Assessment of coronary plaque with optical coherence tomography and high-frequency ultrasound," *Am. J. Cardiol.* **85**(5), 641-644 (2000).
- [7] J. C. Yin, H. C. Yang, X. Li, J. Zhang, Q. F. Zhou, C. H. Hu, K. K. Shung and Z. P. Chen, "Integrated intravascular optical coherence tomography ultrasound imaging system," *J. Biomed. Opt.* **15**(1), 010512 (2010)
- [8] H. C. Yang, J. C. Yin, C. H. Hu, J. Ca--nna, Q. F. Zhou, J. Zhang, Z. P. Chen and K. K. Shung, "A Dual-Modality Probe Utilizing Intravascular Ultrasound and Optical Coherence Tomography for Intravascular Imaging Applications," *IEEE Trans. Ultrason. Ferroelectr. Freq. Control.* **57**(12), 2839-2843 (2011)
- [9] X. Li, J. Yin, C. Hu, Q. Zhou, K. K. Shung, and Z. Chen, "High-resolution coregistered intravascular imaging with integrated ultrasound and optical coherence tomography probe," *Appl. Phys. Lett.* **97**(13), 133702 (2010).
- [10] J. Yin, X. Li, J. Jing, J. Li, D. Mukai, S. Mahon, A. Edris, K. Hoang, K. K. Shung, M. Brenner, J. Narula, Q. Zhou, and Z. Chen, "Novel combined miniature optical coherence tomography ultrasound probe for in vivo intravascular imaging," *J. Biomed. Opt.* **16**(6), 060505 (2011).